

Ci-bo LOU, Li-qin TANG, Dao-hong SONG, Xiao-sheng WANG,
Jing-jun XU, Zhi-gang CHEN

Novel spatial solitons in light-induced photonic bandgap structures

© Higher Education Press and Springer-Verlag 2008

Abstract The study of wave propagation in periodic systems is at the frontiers of physics, from fluids to condensed matter physics, and from photonic crystals to Bose-Einstein condensates. In optics, a typical example of periodic system is a closely-spaced waveguide array, in which collective behavior of wave propagation exhibits many intriguing phenomena that have no counterpart in homogeneous media. Even in a linear waveguide array, the diffraction property of a light beam changes due to evanescent coupling between nearby waveguide sites, leading to normal and anomalous discrete diffraction. In a nonlinear waveguide array, a balance between diffraction and self-action gives rise to novel localized states such as spatial “discrete solitons” in the semi-infinite (or total-internal-reflection) gap or spatial “gap solitons” in the Bragg reflection gaps. Recently, in a series of experiments, we have “fabricated” closely-spaced waveguide arrays (photonic lattices) by optical induction. Such photonic structures have attracted great interest due to their novel physics, link to photonic crystals, as well as potential applications in optical switching and navigation. In this review article, we present a brief overview on our experimental demonstrations of a number of novel spatial soliton phenomena in light-induced photonic bandgap structures, including self-trapping of fundamental discrete solitons and more sophisticated lattice gap solitons. Much of our work has direct impact on the study of similar discrete

phenomena in systems beyond optics, including sound waves, water waves, and matter waves (Bose-Einstein condensates) propagating in periodic potentials.

Keywords solitons, vortices, gap solitons, photonic lattices, bandgap structures, photorefractive

PACS numbers 42.65.Tg, 42.65.Tg, 42.65.Sf, 42.65.Wi, 42.82.Et

1 Introduction

In the last several years, there has blossomed an interest in the study of collective behavior of wave propagation in closely-spaced nonlinear waveguide arrays [1, 2]. Even in linear propagation, the diffraction property of a light beam in the waveguide array (called discrete diffraction) is distinctively different from that in homogeneous media. When the nonlinear effect of the light beam becomes significant, a balance between discrete diffraction and nonlinear self-focusing gives rise to localized states of light better known as “discrete solitons” [3]. Discrete solitons (DSs) have been predicted to exist in a variety of other nonlinear systems such as biology, solid state physics, and Bose-Einstein condensates, but a convenient way to demonstrate such soliton states is to employ a fabricated or optically-induced waveguide array in nonlinear optics. Indeed, the first experimental demonstration of DSs was carried out in fabricated one-dimensional (1D) AlGaAs semiconductor waveguide arrays [4, 5]. Later, it was suggested that DSs could also form in optically-induced waveguide arrays [6]. This soon led to various experimental observations of DSs in such waveguide arrays established with coherent

Ci-bo LOU, Li-qin TANG, Dao-hong SONG, Xiao-sheng WANG,
Jing-jun XU, Zhi-gang CHEN (✉)

The Key Laboratory of Weak-Light Nonlinear Photonics, Ministry of Education and TEDA Applied Physical School, Nankai University, Tianjin 300457, China
E-mail: zgchen@nankai.edu.cn

Received December 20, 2007; accepted December 30, 2007

multi-beam interference [7–9] or amplitude modulation of a partially coherent beam [10, 11]. In addition to fundamental discrete solitons, vortex discrete solitons have also been predicted theoretically [12–15] and demonstrated experimentally [16, 17]. In all these studies, the localization of a probe beam in uniform periodic structures results from the combined effect of lattice discreteness and nonlinear self-trapping, and the formation of a DS could be considered as a self-induced *nonlinear* photonic defect mode formed in the semi-infinite gap of the lattices due to total internal reflection.

On the other hand, it is well known that optical periodic structures offer many unique and interesting features due to the existence of the photonic band-gap (PBG). One example is a fundamentally different way of waveguiding by defects in otherwise uniform periodic structures as opposed to conventional guidance by total internal reflection or soliton-induced nonlinear self-guiding. Such a waveguiding property has been demonstrated previously mainly with photonic crystals, where guidance is associated with the formation of time-domain frequency defect modes [18–29]. Recently, similar analyses of how a monochromatic light field distributes in waveguide lattices has been focused on the bandgaps of spatial frequency modes (i.e., propagation constant vs. transverse wave vector) [30–32]. Localization of a light beam results from bandgap guidance or the formation of *linear* space-domain frequency defect modes has been demonstrated in a number of experiments [33–39].

In addition to nonlinear “discrete solitons” and linear photonic bandgap guidance, the optical periodic structure also provides a platform for studying nonlinear wave localized in a “true” photonic bandgap, even if the periodic lattice structure itself is uniform, i.e., without structured defects. For instance, in a nonlinear waveguide lattice, a balance between discrete diffraction and nonlinear self-action can give rise to localized states of light better known as spatial “gap solitons” [40–44], which bifurcate from Bloch modes but have their propagating constants located within a Bragg reflection gap (e.g., between the first and second optical Bloch Bands or in a higher bandgap). These gap soliton states can be achieved with either self-focusing nonlinearity [42, 43] or self-defocusing nonlinearity [41, 44], and can be observed with off-axis excitations in which the probe beam is launched at an angle to match the edge of the first Brillouin Zone [41] or with on-axis excitations without *a priori* spectral or phase engineering as demonstrated in our recent experiment [44]. Recently, we have also demonstrated a new type of discrete soliton states different from all previously observed gap solitons, namely, “embedded solitons”, for which the soliton propagating constants reside within a

photonic Bloch band rather than a Bragg reflection gap.

In this review article, we present a brief overview on our experimental work of novel spatial solitons in two-dimensional light-induced photonic lattices, including self-trapping of discrete solitons in the semi-infinite gap with self-focusing nonlinearity, and lattice spatial gap solitons in the Bragg reflection gap with self-defocusing nonlinearity. We discuss briefly how to “fabricate” these lattices by the method of optical induction, and how to demonstrate the formation of discrete solitons and discrete vortex solitons in focusing lattices. We then focus on our recent work on fundamental and dipole-like high-order lattice gap solitons, discrete gap soliton trains, and gap vortex solitons in self-defocusing lattices. Our optical induction of reconfigurable photonic lattices with “reversible” nonlinearity not only has a direct link to technologically important systems of periodic structures such as photonic crystals, but also brings about the possibility for studying many novel phenomena in periodic systems beyond optics in a simply optical setting. For instance, there have been an increasing interest in the study of localized soliton states in condensed matter physics and BECs, for which the results from nonlinear optics have certainly provided synergetic idea and insight.

2 “Fabrication” of 2D self-focusing and -defocusing photonic lattices

With today’s nano-fabrication technology, to create a closely-spaced 1D waveguide array on a substrate material is not a problem. As an example, such waveguide structures have been fabricated with AlGaAs semiconductor materials or LiNbO₃ crystals. In fact, the first experimental demonstration of DSs was carried out in fabricated 1D semiconductor waveguide arrays [4, 5]. Yet, it has always been a challenge to create or fabricate 2D or 3D waveguide arrays in bulk media. Motivated by observation of DSs in higher dimensions, it has been suggested that waveguide lattices could be optically-induced in a photorefractive crystal [6]. Indeed, experimental observations of DSs in such waveguide lattices were established with optical induction by sending multiple interfering beams into the nonlinear crystal [7–9]. However, the coherent multiple-beam interference method has many disadvantages for creating photonic lattice structures. For instance, the induced lattice tends to be more sensitive to ambient perturbation. Furthermore, when the lattice beam itself experiences an appreciable nonlinearity, it becomes considerably more susceptible to modulation instability and the lattice structure cannot be

stable either when the lattice spacing is too small or the nonlinearity is too high. More importantly, the interference method cannot generate more complicated lattice structures such as binary lattices or lattices with structured defects. In view of that, we proposed a different method of optical induction which is based on the periodic amplitude modulation of a partially coherent optical beam. This incoherent amplitude-modulation method made possible the first experimental demonstration of 2D solitonic lattices in a 3D bulk crystal [45, 46]. In what follows, we describe our experimental arrangement for the lattice induction, for both self-focusing and defocusing lattices.

The experimental setup for our study is illustrated in Fig.1. Our experiments are typically performed in a biased SBN:60 photorefractive crystal illuminated by a laser beam ($\lambda = 488 \text{ nm}$ or $\lambda = 532 \text{ nm}$) passing through a rotating diffuser and an amplitude mask. The biased crystal (bias field can vary from -1.6 to 6.0 kV/cm) provides a self-focusing or defocusing noninstantaneous nonlinearity [47]. To generate a 2D-waveguide lattice, we use an amplitude mask to spatially modulate (in two orthogonal transverse directions) the otherwise uniform incoherent beam after the diffuser. The rotating diffuser turns the laser beam into a partially spatially incoherent beam with controllable degree of spatial coherence, as first introduced in experiments with incoherent optical solitons [48–50]. The mask is then imaged onto the input face of the crystal, thus creating a pixel-like input intensity pattern which remains stationary through the crystal after proper spatial filtering [45, 46]. This lattice beam can be turned into either extraordinarily or ordinarily polarized with a half-wave plate as necessary. Another beam, either split from the same laser or emitted from a different laser and which does not pass through the diffuser and the

mask, is used as our probe beam or soliton-forming beam, propagating collinearly with the lattice. Different excited cases will be illustrated in following sections. As explained below, both the lattice beam and the probe beam can be made to undergo linear or nonlinear propagation through the biased crystal by adjusting their intensity, polarization, or wavelengths. The two beams are monitored separately with a CCD camera at the input and output facets of the crystal. To confirm the phase distribution of probe beam, a weak reference beam is introduced to interfere with the probe beam after it exits the crystal (bottom path of the Fig.1). In addition, a white-light background beam illuminating from the top of the crystal is typically used for fine-tuning the photorefractive nonlinearity [45–50].

We emphasize that the method of optical induction of waveguide lattices and nonlinear self-trapping of discrete solitons in photorefractive crystals is directly related to the anisotropic property of the photorefractive nonlinearity. In general, in an anisotropic photorefractive crystal, the nonlinear index change experienced by an optical beam depends on its polarization as well as on its intensity. Under appreciable bias conditions, i.e., when the photorefractive screening nonlinearity is dominant, this index change is approximately given by $\Delta n_e = [n_e^3 r_{33} E_0 / 2](1+I)^{-1}$ and $\Delta n_o = [n_o^3 r_{13} E_0 / 2](1+I)^{-1}$ for extraordinarily-polarized (e-polarized) and ordinarily-polarized (o-polarized) beams respectively [6–11]. Here E_0 is the applied electric field along the crystalline c -axis (x -direction), it can be positive or negative corresponding to self-focusing and self-defocusing nonlinearity cases respectively, and I is the intensity of the beam normalized to the background illumination. Due to the difference between the nonlinear electro-optic coefficients r_{33}

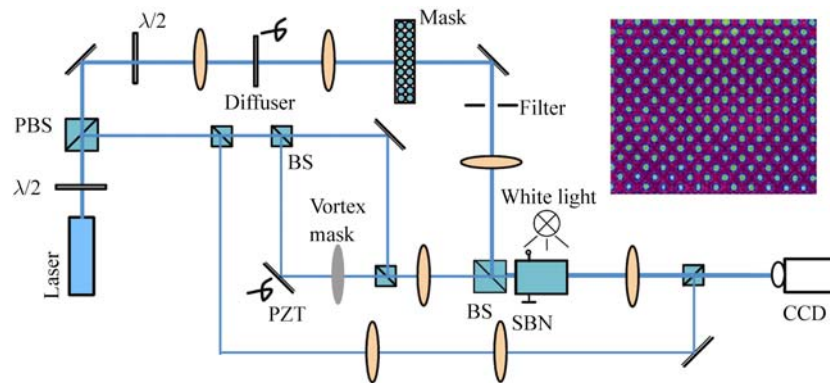


Fig. 1 Experimental setup for optical induction of waveguide lattices in a biased photorefractive crystal by amplitude modulation of a partially coherent beam. PBS: polarizing beam splitter; SBN: strontium barium niobate; PZT: piezoelectric transducer. Top path is the lattice beam, middle path is the probe beam (either a Gaussian or vortex beam with the vortex mask inserted, or can be separated by a Mach-Zehnder interferometer into two beams with controlled relative phase), and bottom path is the reference beam for interference with the probe beam after crystal. The white-light is used as background illumination for fine-tuning the photorefractive nonlinearity. The right insert shows a typical picture of 2D photonic lattice created by optical induction.

and r_{13} , Δn_e is more than 10 times larger than Δn_o under the same experimental conditions in a SBN:60 crystal. Thus, if the lattice beam is o-polarized while the probe beam is e-polarized, the lattice beam would experience only weak nonlinear index change, and, in this case, could be considered as undergoing *linear* propagation. In all our work with discrete solitons and gap solitons, the lattice beam is always o-polarized, thus the lattice beam induces a weak index change for the waveguide arrays. On the other hand, the probe beam is always a coherent e-polarized beam, but its intensity and/or wavelength can be adjusted so it can undergo linear propagation (for study of linear guidance or linear defect modes) or nonlinear propagation (for study of nonlinear trapping as discussed in this paper). We also mention that, by use of the anisotropic property of the photorefractive nonlinearity, it is possible to establish discrete and gap solitons in a nonconventionally biased crystal, where the applied electric field E_0 can be orthogonal rather than parallel to the crystalline c -axis [84, 85].

Typical examples of 2D square lattices created by optical induction in our crystal with both o-polarized and e-polarized beams are shown in Fig. 2. Our experiment shows that the linear square lattices generated with

o-polarized partially coherent beams are stable and robust, even at small lattice spacing of 20 μm or less [Fig. 2 (a)]. However, to create a nonlinear (solitonic) square lattice with the e-polarized beam, it is a challenge to obtain a stable lattice without distortion at such small lattice spacing. In addition, due to the anisotropic self-focusing nonlinearity, the pixels (or waveguides) tend to merge in the y -direction if the square lattice is orientated in horizontal/vertical directions. The diagonal orientation of the square lattice (i.e., its principal axes orientated in the 45° directions relative to x - and y -axis) favors stable lattice formation due to enlarged y -separation between pixels. When the lattice spacing is small, the size of each soliton pixel is also small. With the photorefractive screening nonlinearity, the formation of solitons must satisfy certain conditions better described by the soliton-existence curve [51, 52]. In essence, forming a smaller soliton requires a higher nonlinearity, which is usually achieved by increasing the bias field, which in turn tends to lead to stronger modulation instability as driven by noise such as defects and striations in the crystal. This is why we introduce partial coherence in the lattice beam. As has been previously predicted [53] and experimentally

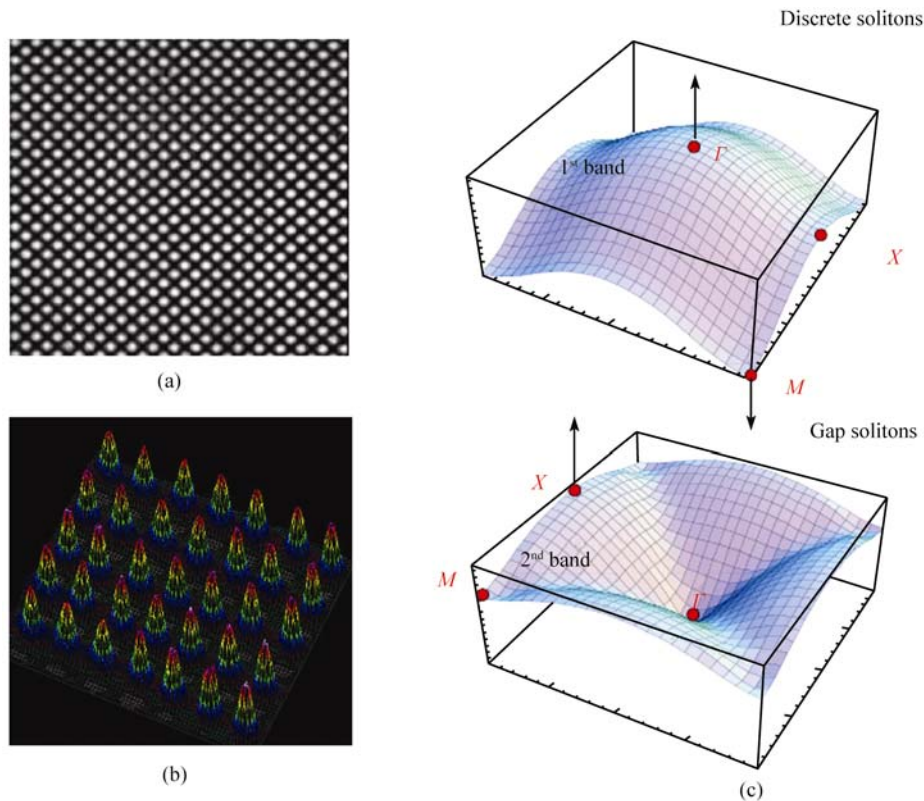


Fig. 2 Optically induced 2D square lattices by amplitude modulation of a partially coherent beam in a biased photorefractive crystal. (a) shows a 2D linear lattice with lattice spacing of 20 μm . (b) shows a typical 3D plots of the 2D nonlinear lattice (with lattice spacing 70 μm) formed as arrays of pixel-like spatial solitons [45, 46]. (c) illustrates the bandgap structure for the first two optical Bloch bands of the 2D square lattices with high-symmetry points within the first Brillouin-zone marked by red dots.

demonstrated [54–59], partial coherence can result in suppression of modulation instabilities. At larger lattice spacing, nonlinear lattices of pixel-like spatial solitons were indeed realized in our earlier experiments. Figure 2 (b) shows a typical example of a stable nonlinear lattice (at $70\ \mu\text{m}$ spacing) obtained by the method of incoherent amplitude modulation [45, 46]. In fact, nonlinear solitonic lattices with spacing as small as $37\ \mu\text{m}$ were realized in our later experiments by fine-tuning the nonlinearity [60]. We show the bandgap structure of the 2D square lattices in Fig. 2 (c), where typical bifurcating high-symmetry points from the first and second Bloch bands leading to discrete and gap solitons are illustrated.

3 Demonstration of nonlinear trapping of discrete solitons in self-focusing lattices

In what follows, we shall use a *linear* square lattice induced with self-focusing nonlinearity for experimental demonstration of spatial discrete solitons. For fundamental 2D discrete solitons [10], the probe beam is focused with a circular lens into a 2D Gaussian beam and launched into one of the lattice sites, while for demonstrating 1D discrete soliton trains [11], the beam is focused with a cylindrical lens into a quasi 1D stripe beam. In experiments with dipole and vector lattice solitons, the probe beam is split into two by a Mach-Zehnder interferometer. The two beams exiting from the interferometer are combined with the lattice beam, propagating collinearly through the crystal. When the two beams from the interferometer are made mutually incoherent by ramping a piezo-transducer mirror at a fast frequency, the vector components are realized by overlapping the two beams onto the same lattice site, where each beam itself is coherent and experiences a strong self-focusing nonlinearity [61]. When the two beams from the interferometer are made mutually

coherent with a controlled phase relation, dipole-like discrete solitons are investigated by launching the two in-phase or out-of-phase beams into two neighboring lattice sites [62]. If the two probe beams are launched into two inter-site locations (i.e., two off-site locations), they can also form symmetric or anti-symmetric (twisted) soliton states depending on their relative phase [63]. For the vortex lattice solitons, the probe beam is sent through a vortex mask, and then launched into the lattice with the vortex ring covering several neighboring lattice sites, as for fundamental vortex, high-order vortex and necklace-like vortex solitons [16, 73, 76]. Below we show some examples of such discrete solitons.

3.1 Discrete fundamental solitons

First, we present our results on 2D fundamental discrete solitons. A stable waveguide lattice (spacing $20\ \mu\text{m}$ and the FWHM of each lattice site about $10\ \mu\text{m}$) is induced by an o-polarized partially coherent beam. Then, a probe beam (whose intensity is 4 times weaker than that of the lattice) is launched into one of the waveguide channels, propagating collinearly with the lattice. Due to weak coupling between closely spaced waveguides, the probe beam undergoes discrete diffraction when the nonlinearity is low, whereas it forms a 2D discrete soliton at an appropriate level of high nonlinearity. Typical experimental results are presented in Fig. 3, where the first two photographs show the Gaussian-like probe beam at the crystal input [Fig. 3 (a)] and its linear diffraction at the crystal output after 8 mm of propagation [Fig. 3 (b)]. Discrete diffraction in the square lattice is observed at a bias field of $900\ \text{V/cm}$ [Fig. 3 (c)], clearly showing that most of the energy flows from the center towards the diagonal directions of the lattice. Even more importantly, a DS is observed at a bias field of $3000\ \text{V/cm}$ [Fig.

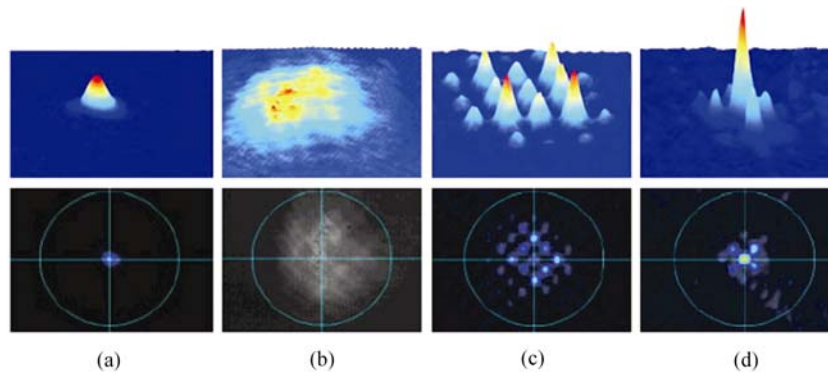


Fig. 3 Experimental demonstration of a discrete soliton in a partially coherent lattice. (a) Input, (b) diffraction output without the lattice, (c) discrete diffraction at $900\ \text{V/cm}$, and (d) discrete soliton at $3000\ \text{V/cm}$. *Top*: 3D intensity plots; *Bottom*: 2D transverse patterns. (after Ref. [10], and animation of the experimentally observed process can be viewed in Ref. [64])

3 (d)], with most of energy concentrated in the center and the four neighboring sites along the principal axes of the lattice. These experimental results are in excellent agreement with expected behavior from the theory of discrete systems [64, 65].

3.2 Discrete two-component composite solitons

Among self-localized states in periodic structures, discrete vector solitons make up an important family. Although vector solitons have been realized previously in continuum nonlinear systems, they were observed only recently in a discrete system of one dimensional AlGaAs waveguide arrays [66]. We demonstrate that two mutually incoherent beams can lock into a fundamental vector soliton while propagating along the same lattice site, although each beam alone would experience discrete diffraction under the same conditions. Such mutually-trapped two-component vector solitons are attributed to the intensity-dependent nonlinearity [61]. By launching two mutually coherent beams (with controlled phase relationship) into two neighboring lattice sites of the square lattice rather than overlapping them in the same lattice site, we have also demonstrated the formation of dipole solitons in a 2D optically induced photonic lattice [62].

In addition to on-site excitation of the probe beams, we have also studied off-site excitations in weakly-coupled lattices created by optical induction. When a weak Gaussian-like probe beam is launched between two lattice sites, its energy switches mainly to the two closest waveguide

channels evenly, leading to a symmetric beam profile. However, as the intensity of the probe beam exceeds a threshold value, the probe beam evolves into an asymmetric beam profile, akin to that resulting from the symmetry breaking in a double-well potential [67]. Should the probe beam itself experience no or only weak nonlinearity (e.g., the probe is at a photo-insensitive wavelength such as 633 nm), such symmetry breaking in the beam profile does not occur regardless the increase of its intensity. When two probe beams are launched in parallel into two off-site locations, they form symmetric or anti-symmetric (dipole-like twisted [9, 62, 68]) soliton states depending on their relative phase as shown in Fig.4. Our experimental and theoretical studies show that both symmetric states (corresponding to a single beam on-site) and anti-symmetric states (corresponding to two out-of-phase beams on two different sites) can be linearly stable [63].

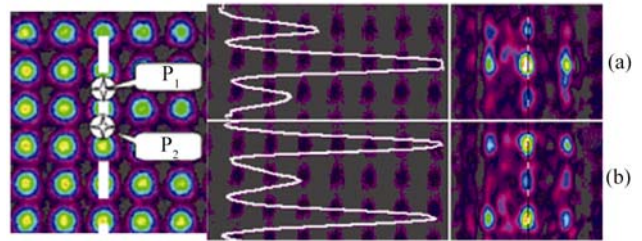


Fig. 4 Formation of symmetric and anti-symmetric (twisted) soliton states for inter-site probing with two mutually coherent beams. Shown are the illustration of probe beam locations (P_1 and P_2) in the lattice (*left*), the combined output beam profile (*middle*), and the intensity pattern (*right*) for in-phase (**a**) and out-of-phase (**b**) excitations. (after Ref. [63])

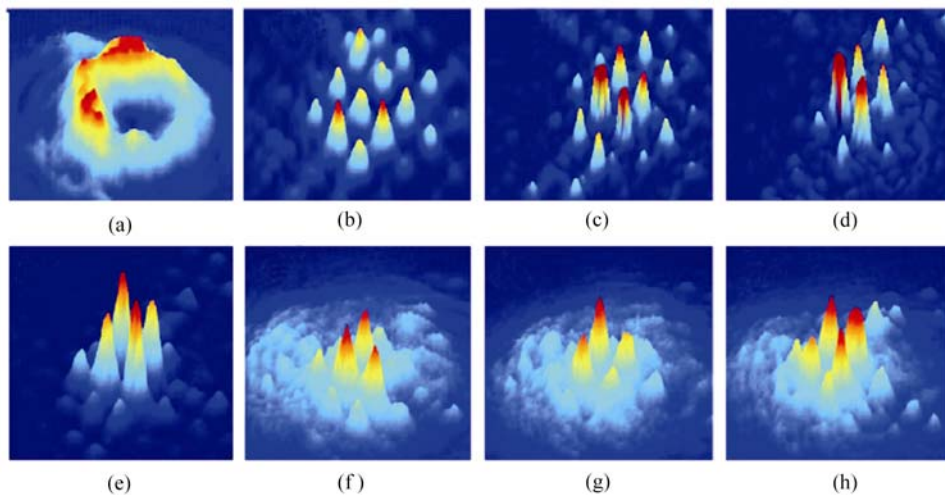


Fig. 5 Formation of a singly-charged ($m=1$) discrete vortex soliton in a 2D photonic lattice. Top panel shows the 3D intensity plots of the vortex beam at crystal output of normal diffraction without the lattice (**a**), output of discrete diffraction at low nonlinearity [(**b**), (**c**)], and output of discrete soliton at high nonlinearity (bias field: 3000 V/cm). The lattice spacing is 28 μm . Bottom panel shows discrete vortex soliton reproduced in a lattice of 20 μm spacing (**e**), and a series of interferogram between the vortex soliton and a weak plane wave (**f**)–(**h**), confirming the nontrivial $\pi/2$ step-phase structure of the vortex at different orientations. (after Ref. [16])

3.3 Discrete vortex solitons

Optical vortex solitons have been demonstrated earlier with continuous media in a number of experiments [69–71], and the basic properties of vortices and vortex solitons can be found in a recent review article [72]. However, vortex solitons propagating in photonic lattices have been demonstrated only recently. Here we present our experimental results of discrete vortex solitons. In this case, the lattice beam is o-polarized while the vortex beam is e-polarized. Typical experimental results on discrete trapping of the vortex with unit topological charge ($m = 1$) are shown in Fig. 5, for which a waveguide lattice with 28 μm spacing is created. The vortex beam [normal diffraction shown in Fig. 5 (a)] is then launched straight into the middle of the four lattice sites, so that the vortex center sits right in the middle of four lattice sites (off-site excitation [13–16]). Due to waveguide coupling, the vortex beam undergoes discrete diffraction when the nonlinearity is low [Fig. 5 (b)–(c)], but it evolves into a discrete vortex soliton at an appropriate level of high nonlinearity [Fig. 5 (d)], with most of the energy concentrated at the central four sites along the principal axes of the lattice. To confirm the nontrivial phase of the vortex soliton, a weak reference beam is introduced to interfere with the discrete vortex after it exits the crystal. We use a piezo-transducer mirror in the reference beam path in order to control its phase relative to the vortex beam. As we actively move the PZT mirror, a series of interferograms are recorded to reconstruct the phase of the vortex. Examples of the interferograms are presented in Fig. 5 (f)–(h), which show that one of the four lobes increases its intensity and the corresponding diagonal lobe decreases its intensity. Furthermore, the lobe with the strongest intensity is alternating among the four spots. These interferograms confirm that the four lobes of the output vortex have a nontrivial phase relation (a $\pi/2$ phase ramp), as expected for the discrete vortex soliton.

4 Demonstration of nonlinear trapping of gap solitons in self-defocusing lattices

Most of the experimental work on discrete solitons has been performed in self-focusing square lattices. Another more fundamental phenomena in periodic media is gap soliton. In photonic lattice, spatial gap solitons [40] can arise from Bloch modes in the first band (close to high-symmetry M points [Fig. 2 (c), top], i.e., the edges of the first Brillouin zone), where anomalous diffraction is counteracted by self-defocusing nonlinearity [8, 77, 78], or the second band (close to X points [Fig. 2 (c), bottom]), where normal dif-

fraction is balanced by self-focusing nonlinearity [42, 43]. We report the experimental demonstration of spatial gap solitons for the first case in a 2D optically induced “backbone” lattice [8, 44] with a saturable self-defocusing nonlinearity. The experimental setup for gap soliton study is similar to those used for discrete solitons [Fig. 1]. In what follows, we discuss spatial gap solitons in defocusing lattices.

4.1 Discrete fundamental gap solitons

First, we summarize our results of on-axis excitation of a single 2D gap soliton in Fig. 6. Different from previous experimental observations in which either the probe beam was launched off-axis to match the edge of the first BZ [41] or its input phase or spectrum was engineered [77], we demonstrate on-axis excitation of a 2D gap soliton without a priori phase or spectral engineering.

In fact, we show that nonlinear trapping of the probe beam leads to spectrum reshaping even though its initial spectrum is nearly uniform in the entire first BZ [Fig. 6 (d)]. The probe beam is focused into a 2D circular beam and launched into one of intensity minima (index maxima) of the “backbone” lattice (with about 23 μm spacing) [Fig. 6 (a)]. The top panels of Fig. 6 show the input lattice beam, its Fourier spectrum, and its band structure of first Bloch band, and the spectrum of probe beam at output after linear propagation through the lattice, respectively. Under linear propagation, the probe beam experiences discrete diffraction, and its spectrum covers the first BZ with most of the power concentrating in the center [Fig. 6 (d)]. The middle panels show the formation of a 2D gap soliton under nonlinear propagation at a bias field of -1.3 kv/cm. The interferograms [Fig. 6 (f), (g)] show clearly that the gap soliton has a staggered phase structure (i.e. the central peak is out-of-phase with neighboring peaks), while its power spectrum [Fig. 6 (h)] reshapes to have most of its power located in the four corners of the first BZ where diffraction is anomalous. These experimental results are corroborated with our numerical simulations using parameters close to those from experiment, as shown in the bottom panel of Fig. 6.

4.2 Two-component dipole-like gap solitons

For multipole gap lattice solitons in 2D self-defocusing lattices, we now report our work on formation of dipolelike gap solitons. Our motivation is to illustrate the similarity and difference in comparison with their counterparts in the focusing case. The dipole-like structures (with two peaks) excited at the intensity minima (index maxima) of the 2D

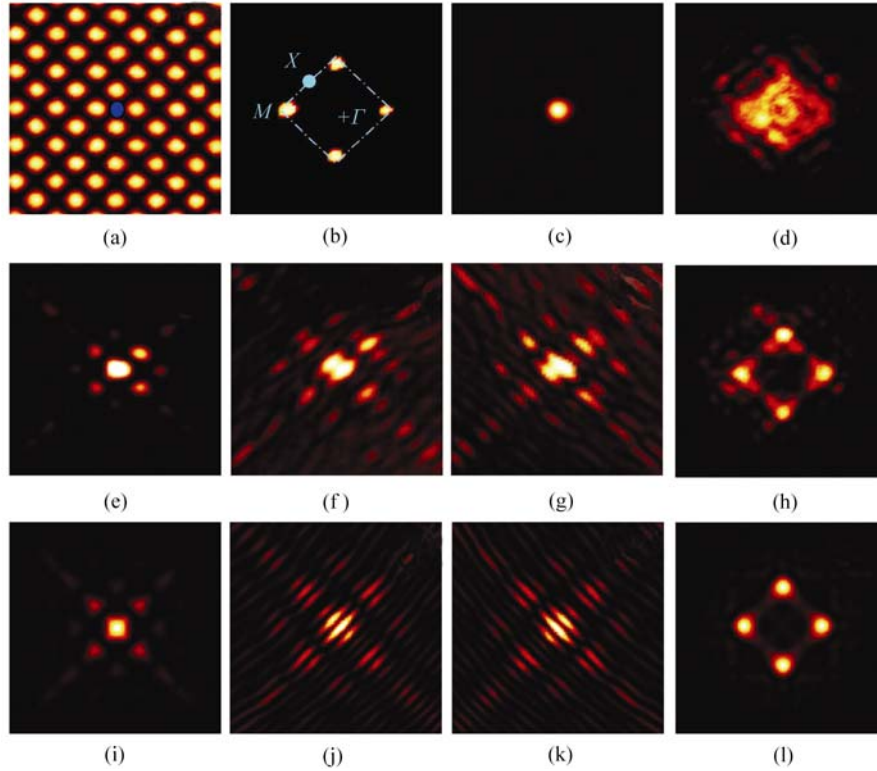


Fig. 6 2D gap soliton by single-beam on-axis excitation. Experimental results (a)–(h) show the lattice pattern with probe-beam input location marked with a blue circle (a), spectrum of lattice with the first BZ and high symmetry points marked (b), probe beam at input (c), probe beam linear output spectrum (d) through the lattice, output pattern of the gap soliton (e), its interferograms with a plane wave tilted from two different directions (f), (g) and its nonlinear output spectrum (h). Bottom panel: Numerical results (i)–(l) show the gap soliton formation corresponding to (e)–(h).

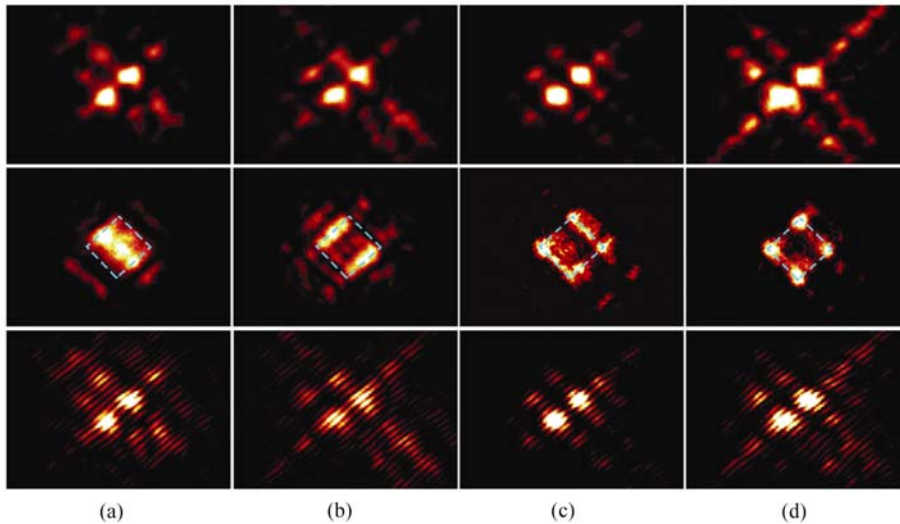


Fig. 7 Experimental results on IP [(a), (b)] and OOP [(c), (d)] dipole-like gap solitons under diagonal excitation. Shown are output patterns (top), corresponding Fourier spectra (middle), and interferograms (bottom) for linear [(a), (c)] and nonlinear [(b), (d)] propagation. (after Ref. [86])

“backbone” lattice with 25 μm spacing. The two intensity peaks can be in phase (IP) or out-of-phase (OOP), and they are located in two nearest waveguide sites (e.g., diagonal excitation along one direction of the principal axes). For this

experiment, again the lattice beam is o-polarized while the dipole beam is e-polarized. Typical experimental results under diagonal excitation are presented in Fig. 7 for both the IP and the OOP cases. We do not see significant difference

in intensity patterns between the linear [Fig. 7 (a), (c)] and nonlinear [Fig. 7 (b), (d)] cases simply because of the reduced coupling. However, remarkable differences can be seen in the spectrum and the phase structure of the dipole “tails”. Due to constructive interference, the linear spectrum of IP dipole covers the first BZ with most of the power concentrating in the center, while the diagonally excited OOP dipole covers the four M points. Under a bias field of -1.1 kV/cm, however, for the IP dipole the nonlinear spectrum reshapes and the energy transfers from the central region (normal diffraction) towards two lateral regions close to the two X points; for the OOP case the spectrum reshapes and the energy transfers quickly to the regions close to the four M points where diffraction is anomalous. We visualize the phase structure of the dipole beam by taking its interference pattern with a tilted broad beam. The initial structures for both cases are preserved in the central two peaks, while the tails along the dipoles direction show signs of OOP relation between adjacent peaks as the fringes tend to break and shift, as if to match the Bloch modes at the M points of the first band which have a checkerboard phase structure [79]. More detailed experimental and theoretical results of this work can be found in our recent publication [86].

4.3 Discrete gap soliton trains

Note that we have demonstrated gap solitons localized mainly in a single spot or two spots corresponding to the waveguide lattice sites, is that possible to create a train of gap solitons that would populate many lattice sites? The answer can be found in our recent experimental demonstration of a gap soliton train excited by a uniform stripe beam. The superimposed intensity pattern of the lattice and stripe

beam at input is shown in Fig. 8 (a). The vertically oriented stripe beam propagates collinearly with the lattice. Their power spectra are shown in Fig. 8 (b), where the spectrum of the stripe beam forms nearly a horizontal line extended to two diagonal M points of the square lattice. Under nonlinear propagation at a bias field of -1.6 kV/cm, the stripe beam evolves into a gap soliton train [Fig. 8 (c)], similar to that found in our theoretical model [44]. The staggered phase structure of the soliton beam is confirmed by its interferograms with a tilted plane wave [Fig. 8 (d)], where the breaking and interleaving of interference fringes suggests the out-of-phase relation between the central stripe and two lateral stripes. Careful experimental and theoretical studies indicate that the power spectrum of the probe beam has been drastically reshaped by nonlinear trapping [44]. This work is important not only because that the gap soliton train we generated could be considered as nonlinearity-induced line defects in photonic band gap structure, but we have predicted and demonstrated the formation of a new type of “unexpected” gap soliton trains due to nonlinear transport and spectrum reshaping of a stripe beam in 2D induced lattices. The soliton trains arise from Bloch modes from the high-symmetry M points of the first photonic band, although some of these modes are initially not or only weakly excited from lattice scattering or diffraction. These results may have direct impact on the study of nonlinear Bloch-wave interaction and localization in periodic systems beyond optics such as condensed matter physics or Bose-Einstein condensates, where 2D gap solitons might arise from electronic/atomic Bloch modes weakly populated in the ground state by quantum fluctuations even if complete preparation of coherent wave packets at the corresponding band edge is not feasible.

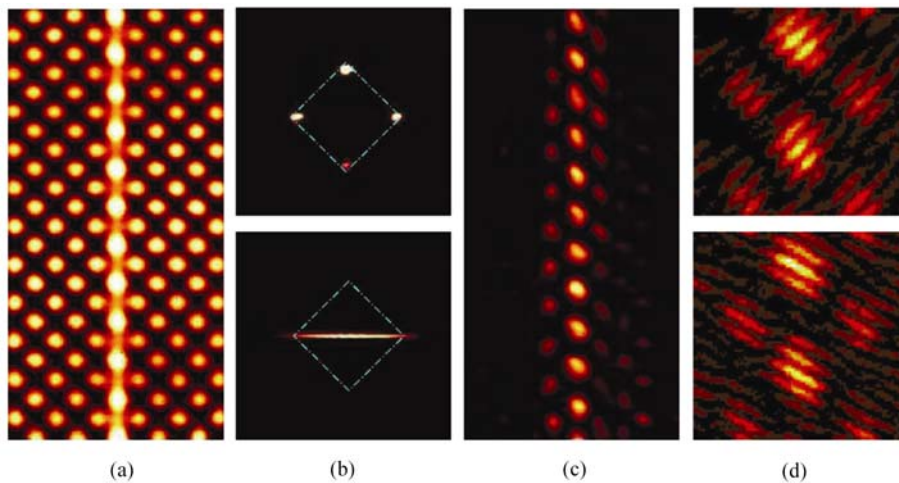


Fig. 8 Experiment results showing formation of a gap soliton train. (a) Superimposed pattern of a vertically-oriented stripe beam and the lattice beam at input; (b) Input spectrum of the lattice (*top*) and probe (*bottom*) beam with the first BZ marked by dotted line; (c) Output pattern of the gap soliton train and its interferograms with a plane wave tilted from two different directions (d). (after Ref. [44])

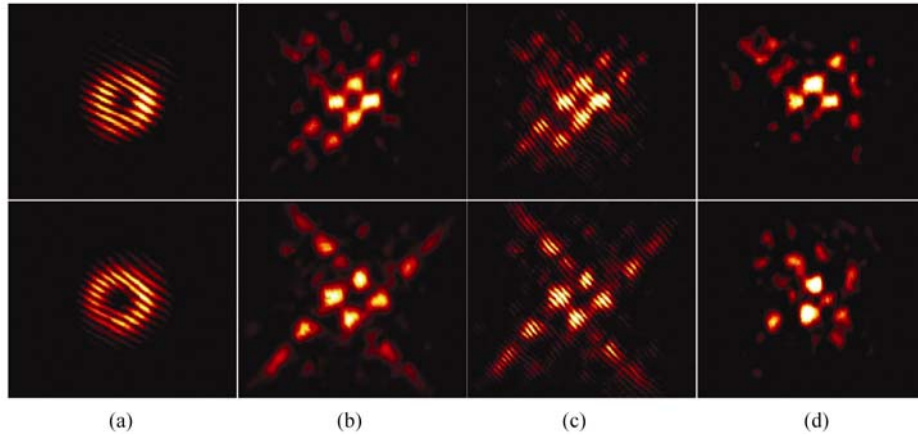


Fig. 9 Experimental demonstration of self-trapping of singly-charged (*top*) and doubly-charged (*bottom*) vortices in a defocusing photonic lattice. **(a)** Interferogram showing the phase of the vortex beam, **(b)** self-trapped vortex pattern, **(c)**, **(d)** interferogram between **(b)** and a tilted plane wave and an on-axis Gaussian beam, respectively.

4.4 Discrete gap vortex solitons

Finally, we present our very recent experimental work on 2D gap vortex solitons by on-axis excitation of a single vortex beam in a self-defocusing “backbone” photonic lattice. We show that a singly-charged ($m = 1$) vortex can evolve into a gap vortex soliton, but a doubly-charged ($m = 2$) vortex tends to turn into a quasi-vortex or quadrupole-like structure. The experimental setup used for this study is similar to that used for observation of discrete (semi-infinite gap) vortex solitons in self-focusing lattices [16], except that we now use self-defocusing lattices as used for generation of above gap solitons. Typical experimental results are summarized in Fig. 9, where off-site excitations (the vortex core on an index minimum) of both $m = 1$ and $m = 2$ vortices are illustrated. The interferograms of the input vortex beam with a plane wave are shown in Fig. 9 (a), confirming the topological charge. Self-trapping of the vortices is achieved at a bias field of about -1.2 kV/cm as shown in Fig. 9 (b). Both singly- and doubly-charged vortices break up primarily into four intensity spots, similar to the discrete vortex solitons [16, 17] but with longer tails along principle axes. In order to identify their phase structures, a tilted plane wave is sent to interfere with the output vortex pattern [Fig. 9 (c)], and it is found that the vortices maintain the helical phase structure after 10 mm of propagation through the crystal. Sending a co-axial broad Gaussian beam as interfering beam, we can see clearly that the phase structures for self-trapped $m = 1$ and $m = 2$ vortices are different [Fig. 9 (d)]. Numerical beam-propagation simulation to longer propagation distance (up to 40 mm) indicates that the phase singularity can maintain for $m = 1$ vortex, but not for $m = 2$ vortex (the latter evolve into a quadrupole structure). We note that self-trap-

ping of doubly-charged ($m = 2$) vortices in self-focusing lattices have been demonstrated in our earlier experiments [73], for which vortex rotation and charge flipping has been observed with the quadrupole formation as a transient state before the charge flipping occurs. Further experimental and theoretical studies are current underway to understand the formation and stability the high-order vortex gap solitons.

5 Summary

In summary, we have successfully “fabricated” by optical induction 2D reconfigurable photonic lattices. These lattices have served as a platform for us to demonstrate a variety of novel spatial solitons in periodic optical structures, which include nonlinear localized states of beam propagation with various geometrical and phase structures in semi-infinite gap or Bragg reflection gap, such as dipole-like discrete or gap solitons, vortex discrete or gap solitons, stripe-shaped discrete or gap soliton trains. The mechanisms for light confinement in these lattice structures include nonlinear discrete self-trapping due to the semi-infinite (or total internal reflection) gap as well as the repeated Bragg reflection (or photonic) bandgaps. Our results pave the way for further study of new phenomena in periodic photonic structures, as well as for exploring potential applications in beam shaping and light routing with reconfigurable lattices.

We close by mentioning that, in this review article, we have provided an overview mainly about our own work on optically-induced photonic lattices and their nonlinear light guiding properties. There are a number of research groups worldwide actively working in this dynamically changing field of nonlinear optics and photonics [80–83]. In addition, more detailed review about our work on lattice induction

and discrete solitons in uniformly structured photonic lattices as well as on linear bandgap guidance of light in induced lattices with structured defects can be found in Refs. [87, 88].

Acknowledgements This work was supported in part by the Major State Basic Research Development Program of China (973 Program), 111 Project, the National Natural Science Foundation of China (NSFC), Program for Changjiang Scholars and Innovative Research Team in University (PCSIRT) in China, and by National Science Foundation (NSF), the Air Force Office of Scientific Research (AFOSR) and the Petroleum Research Funds (PRF). We are indebted to many of our collaborators over the years including J. Yang, D. Kip, D. N. Christodoulides, Y. S. Kivshar, P. G. Kevrekidis, P. Zhang, and to our student co-workers including A. Bezryadina, X. Chen and H. Martin. Z. Chen and X. Wang are also with the Department of Physics and Astronomy, San Francisco State University.

References

1. D. N. Christodoulides, F. Lederer, and Y. Silberberg, *Nature*, 2003, 424: 817
2. D. Campbell, S. Flach, and Y. S. Kivshar, *Phys. Today*, 2004, 57: 43
3. D. N. Christodoulides and R. I. Joseph, *Opt. Lett.*, 1988, 13: 794
4. H. S. Eisenberg, Y. Silberberg, R. Morandotti, A. R. Boyd, and J. S. Aitchison, *Phys. Rev. Lett.*, 1998, 81: 3383
5. R. Morandotti, H. S. Eisenberg, Y. Silberberg, M. Sorel, and J. S. Aitchison, *Phys. Rev. Lett.*, 2001, 86: 3296
6. N. K. Efremidis, S. Sears, D. N. Christodoulides, J. W. Fleischer, and M. Segev, *Phys. Rev. E*, 2002, 66: 046602
7. J. W. Fleischer, T. Carmon, M. Segev, N. K. Efremidis, and D. N. Christodoulides, *Phys. Rev. Lett.*, 2003, 90: 023902
8. J. W. Fleischer, M. Segev, N. K. Efremidis, and D. N. Christodoulides, *Nature*, 2003, 422: 147
9. D. Neshev, E. Ostrovskaya, Y. Kivshar, and W. Krolikowski, *Opt. Lett.*, 2003, 28: 710
10. H. Martin, E. D. Eugenieva, Z. Chen, and D. N. Christodoulides, *Phys. Rev. Lett.*, 2004, 92: 123902
11. Z. Chen, H. Martin, E. D. Eugenieva, J. Xu, and A. Bezryadina, *Phys. Rev. Lett.*, 2004, 92: 143902
12. B. A. Malomed and P. G. Kevrekidis, *Phys. Rev. E*, 2001, 64: 026601
13. J. Yang and Z. H. Musslimani, *Opt. Lett.*, 2003, 28: 2094
14. Z. Musslimani and J. Yang, *J. Opt. Soc. Am. B.*, 2004, 21: 973
15. J. Yang, *New Journal of Physics*, 2004, 6: 47
16. D. N. Neshev, T. J. Alexander, E. A. Ostrovskaya, Y. S. Kivshar, H. Martin, I. Makasyuk, and Z. Chen, *Phys. Rev. Lett.*, 2004, 92: 123903
17. J. W. Fleischer, G. Bartal, O. Cohen, O. Manela, M. Segev, J. Hudock, and D. N. Christodoulides, *Phys. Rev. Lett.*, 2004, 92: 123904
18. J. D. Joannopoulos, R. D. Meade, and J. N. Winn, *Photonic Crystals: Molding the Flow of Light*, Princeton, NJ, 1995
19. P. Russell, *Science*, 2003, 299: 358
20. S. L. McCall, P. M. Platzman, R. Dalichaouch, D. Smith, and S. Schultz, *Phys. Rev. Lett.*, 1991, 67: 2017
21. E. Yablonovitch, T. J. Gmitter, R. D. Meade, A. M. Rappe, K. D. Brommer, and J. D. Joannopoulos, *Phys. Rev. Lett.*, 1991, 67: 3380
22. M. Bayindir, B. Temelkuran, and E. Ozbay, *Phys. Rev. Lett.*, 2000, 84: 2140
23. F. Luan, A. K. George, T. D. Hedley, G. J. Pearce, D. M. Bird, J. C. Knight, and P. St. J. Russell, *Opt. Lett.*, 2004, 29: 2369
24. A. Argyros, T. A. Birks, S. G. Leon-Saval, C. B. Cordeiro, F. Luan, and P. St. J. Russell, *Opt. Express*, 2005, 13: 309
25. J. Schmidtke, W. Stille, and H. Finkelmann, *Phys. Rev. Lett.*, 2003, 90: 083902
26. J. S. Foresi, P. R. Villeneuve, J. Ferrera, E. R. Thoen, G. Steinmeyer, S. Fan, J. D. Joannopoulos, L. C. Kimerling, H. I. Smith, and E. P. Ippen, *Nature(London)*, 1997, 390: 143
27. S. Fan, P. R. Villeneuve, J. D. Joannopoulos, and H. A. Haus, *Phys. Rev. Lett.*, 1998, 80: 960
28. X. Wu, A. Yamilov, X. Liu, S. Li, V. P. Dravid, R. P. H. Chang, and H. Cao, *Appl. Phys. Lett.*, 2004, 85: 3657
29. O. Painter, R. K. Lee, A. Scherer, A. Yariv, J. D. O'Brien, P. D. Dapkus, and I. Kim, *Science*, 1999, 284: 1819
30. D. Mandelik, H. S. Eisenberg, Y. Silberberg, R. Morandotti, and J. S. Aitchison, *Phys. Rev. Lett.*, 2003, 90: 53902
31. N. K. Efremidis, J. Hudock, D. N. Christodoulides, J. W. Fleischer, O. Cohen, and M. Segev, *Phys. Rev. Lett.*, 2003, 91: 213906
32. A. A. Sukhorukov, D. Neshev, W. Krolikowski, and Y. S. Kivshar, *Phys. Rev. Lett.*, 2004, 92: 093901
33. U. Peschel, R. Morandotti, J. S. Aitchison, H. S. Eisenberg, and Y. Silberberg, *Appl. Phys. Lett.*, 1999, 75: 1348
34. R. Morandotti, H. S. Eisenberg, D. Mandelik, Y. Silberberg, D. Modotto, M. Sorel, C. R. Stanley, and J. S. Aitchison, *Opt. Lett.*, 2003, 28: 834
35. F. Fedele, J. Yang, and Z. Chen, *Opt. Lett.*, 2005, 30: 1506
36. F. Fedele, J. Yang, and Z. Chen, *Stud. Appl. Math.*, 2005, 115: 279
37. X. Wang, Z. Chen, and J. Yang, *Opt. Lett.*, 2006, 31: 1887
38. I. Makasyuk, Z. Chen, and J. Yang, *Phys. Rev. Lett.*, 2006, 96: 223903
39. X. Wang, J. Young, Z. Chen, D. Weinstein, and J. Yang, *Opt. Express*, 2006, 14: 7362
40. Y. S. Kivshar, *Opt. Lett.*, 1993, 18: 1147
41. J. W. Fleischer, T. Carmon, M. Segev, N. K. Efremidis, and D. N. Christodoulides, *Phys. Rev. Lett.*, 2003, 90: 023902
42. D. Mandelik, R. Morandotti, J. S. Aitchison, and Y. Silberberg, *Phys. Rev. Lett.*, 2004, 92: 093904
43. D. N. Neshev, A. A. Sukhorukov, B. Hanna, W. Krolikowski, and Y. S. Kivshar, *Phys. Rev. Lett.*, 2004, 93: 083905
44. C. Lou, X. Wang, J. Xu, Z. Chen, and J. Yang, *Phys. Rev. Lett.*, 2007, 98: 213903
45. Z. Chen and K. McCarthy, *Opt. Lett.*, 2002, 27: 2019
46. Z. Chen, K. MacCarthy, and H. Martin, *Optics and Photonic News*, December 2002
47. M. Shih, Z. Chen, M. Mitchell, and M. Segev, *J. Opt. Soc. Am. B*, 1997, 14: 3091
48. M. Mitchell, Z. Chen, M. Shih, and M. Segev, *Phys. Rev. Lett.*, 1996, 77: 490
49. Z. Chen, M. Mitchell, M. Segev, T. H. Coskun, and D. N. Christo-

- doulides, *Science*, 1998, 280: 889
50. Z. Chen, M. Segev, and D. N. Christodoulides, *Journal of Optics A: Pure and Applied Optics*, 2003, 5: S389
 51. M. Segev, G. C. Valley, B. Crosignani, P. DiPorto, and A. Yariv, *Phys. Rev. Lett.*, 1994, 73: 3211
 52. Z. Chen, M. Segev, T. H. Coskun, and D. N. Christodoulides, *Opt. Lett.*, 1996, 21: 1436
 53. M. Soljacic, M. Segev, T. Coskun, D. N. Christodoulides, and A. Vishwanath, *Phys. Rev. Lett.*, 2000, 84: 467
 54. T. H. Coskun, D. N. Christodoulides, Y. -R. Kim, Z. Chen, M. Soljacic, and M. Segev, *Phys. Rev. Lett.*, 2000, 84: 2374
 55. D. Kip, M. Soljacic, M. Segev, E. Eugenieva, and D. N. Christodoulides, *Science*, 2000, 290: 495
 56. J. Klinger, H. Martin, and Z. Chen, *Opt. Lett.*, 2001, 26: 271
 57. Z. Chen, J. Klinger, and D. N. Christodoulides, *Phys. Rev. E*, 2002, 66: 66601
 58. Z. Chen, S. Sears, H. Martin, M. Segev, and D. N. Christodoulides, *Proc. Natl. Acad. Sci. USA*, 2002, 99: 5523
 59. D. Kip, M. Soljacic, M. Segev, S. M. Sears, and D. N. Christodoulides, *J. Opt. Soc. Am. B*, 2002, 19: 502
 60. Z. Chen, H. Martin, A. Bezryadina, D. Neshev, Y. S. Kivshar, and D. N. Christodoulides, *J. Opt. Soc. Am. B*, 2005, 22: 1395
 61. Z. Chen, I. Makasyuk, A. Bezryadina, and J. Yang, *Opt. Lett.*, 2004, 29: 1656
 62. J. Yang, I. Makasyuk, A. Bezryadina, and Z. Chen, *Opt. Lett.*, 2004, 29: 1662
 63. C. Lou, J. Xu, L. Tang, Z. Chen, and P. G. Kevrekidis, *Opt. Lett.*, 2006, 31: 492
 64. Z. Chen, H. Martin, E. D. Eugenieva, J. Xu, J. Yang, and D. N. Christodoulides, *Opt. Express*, 2005, 13: 1816
 65. J. Hudock, N. K. Efremidis, and D. N. Christodoulides, *Opt. Lett.*, 2004, 29: 268
 66. J. Meier, J. Hudock, D. N. Christodoulides, G. Stegeman, Y. Silberberg, R. Morandotti, and J. S. Aitchison, *Phys. Rev. Lett.*, 2003, 91: 143907
 67. P. G. Kevrekidis, Z. Chen, B. A. Malomed, D. J. Frantzeskaki, and M. I. Weinstein, *Phys. Lett. A*, 2005, 340: 275
 68. S. Darmanyan, A. Kobaykov, and F. Lederer, *JETP*, 1998, 86: 682
 69. G. A. Swartzlander and C. T. Law, *Phys. Rev. Lett.*, 1992, 69: 2503
 70. Z. Chen, M. Segev, D. W. Wilson, R. E. Muller, and P. D. Maker, *Phys. Rev. Lett.*, 1997, 78: 2948
 71. Z. Chen, M. Shih, M. Segev, D.W. Wilson, R. E. Muller, and P. D. Maker, *Opt. Lett.*, 1997, 22: 1751
 72. A. S. Desyatnikov, Y. S. Kivshar, and L. Torner, in: *Progress in Optics*, E. Wolf ed., North-Holland, 2005, 47
 73. A. Bezryadina, E. Eugenieva, and Z. Chen, *Opt. Lett.*, 2006, 31: 2458
 74. A. Smerzi, A. Trombettoni, P. G. Kevrekidis, and A. R. Bishop, *Phys. Rev. Lett.*, 2002, 89: 170402
 75. P. G. Kevrekidis, G. Theocharis, D. J. Frantzeskakis, and B. A. Malomed, *Phys. Rev. Lett.*, 2003, 90: 230401
 76. J. Yang, I. Makasyuk, P. G. Kevrekidis, H. Martin, B. A. Malomed, D. J. Frantzeskakis, and Z. Chen, *Phys. Rev. Lett.*, 2005, 94: 113902
 77. F. Chen, M. Stepić, C. Rüter, D. Runde, D. Kip, V. Shandarov, O. Manela, and M. Segev, *Opt. Express*, 2005, 13: 4314
 78. G. Bartal, O. Cohen, O. Manela, M. Segev, J. W. Fleischer, R. Pezer, and H. Buljan, *Opt. Lett.*, 2006, 31: 483
 79. D. Träger, R. Fischer, D. N. Neshev, A. A. Sukhorukov, C. Denz, W. Królikowski, and Y. S. Kivshar, *Opt. Express*, 2006, 14: 1913
 80. Y. S. Kivshar and G. P. Agrawal, *Optical Solitons*, New York: Academic Press, 2003
 81. S. Aitchison, D. Christodoulides, and L. Torner, *J. Opt. Soc. Am. B*, 2005, 22: 1346
 82. D. Christodoulides, *Opt. Express*, 2005, 13: 1761
 83. Y. Kartashov, L. Torner, D. Christodoulides, and V. Vysloukh, *Progress in Optics*, to appear
 84. P. Zhang, J. Zhao, C. Lou, X. Tan, Y. Gao, Q. Liu, D. Yang, J. Xu, and Z. Chen, *Opt. Express*, 2006, 15: 536
 85. P. Zhang, et al., *Appl. Opt.*, 2006, 45: 2273
 86. L. Tang, C. Lou, X. Wang, D. Song, X. Chen, J. Xu, and Z. Chen, H. Susanto and P. G. Kevrekidis, *Opt. Lett.*, 2007, 32: 3011
 87. Z. Chen and J. Yang, *Controlling Light in Reconfigurable Photonic Lattices*, Review Book Chapter, in: *Nonlinear Optics and Applications*, H. Abdeldayem ed., Research Signpost, 2007
 88. J. Yang, X. Wang, J. Wang, and Z. Chen, *Light Localization by Defects in Optically Induced Photonic Structures*, Invited Book Chapter, in: *Nonlinearities in Periodic Structures and Metamaterials*, C. Denz, S. Flach, and Y. Kivshar ed., Springer, 2008